

Supporting Information

A ratiometric fluorescent probe for in vivo tracking of alkaline phosphatase level variation resulted from drug-induced organ damages

Xianfeng Hou, Qingxiang Yu, Fang Zeng,* Junhui Ye, and Shuizhu Wu*

College of Materials Science & Engineering, State Key Lab of Luminescent Materials & Devices, South China University of Technology, Guangzhou 510640, P. R. China.

Experimental Section

Synthesis of 1

Under a nitrogen atmosphere, N,N-dimethylethylenediamine (352 mg, 4 mmol), 4-bromo-1,8-naphthalic anhydride (552 mg, 2 mmol) were dissolved under stirring in ethyl alcohol for 10 min, then heated to 85 °C and refluxed for 5 h. The mixture was cooled and the precipitate was collected by filtration. The product was dried under vacuum at 45 °C overnight as a light yellow powder (yield: 72%). ¹H NMR (CDCl₃, 400 MHz, ppm): 2.36 (s, 6H), 2.66 (t, J = 6.4 Hz, 2H), 4.33 (t, J = 6.8 Hz, 2H), 7.84 (t, J = 6.8 Hz, 1H), 8.05 (d, 1H), 8.40 (d, 1H), 8.56 (d, 1H), 8.65 (d, 1H). MS(ESI): m/z = 348.5 [M+H]⁺.

Synthesis of 2

Under a nitrogen atmosphere, the above-obtained compound **1** (173 mg, 0.5 mmol), sodium methylate (216 mg, 4 mmol) and CuSO₄ · 5H₂O (15mg, 0.06 mmol) were dissolved under stirring in methyl alcohol for 10 min, then heated to 70 °C and refluxed overnight. The cooled mixture was washed with ethyl acetate for six times and dried over anhydrous Na₂SO₄. The solvent then was evaporated and the product was dried under vacuum at 50 °C for 48 h as a light yellow powder (yield: 70%). ¹H NMR (CDCl₃, 400 MHz, ppm): 2.41 (s, 6H), 2.72 (t, J = 6.4 Hz, 2H), 4.14 (s, 3H), 4.36 (t, J = 6.8 Hz, 2H), 7.07 (d, 1H), 7.72 (t, J = 7.2 Hz, 1H), 8.55-8.65 (m, 3H). MS(ESI): m/z = 299.0 [M+H]⁺.

Synthesis of 3

Compound **2** (89 mg, 0.3 mmol) was dissolved in 5 mL HI aqueous solution under

stirring, then heated to 130°C and refluxed overnight. The cooled mixture was adjusted to a faintly acid pH with 5M NaOH and the precipitate was collected by filtration. The product was dried under vacuum at 50 °C for 48 h as a light brown power (yield: 86%). ¹H NMR (d6-DMSO, 400 MHz, ppm): 2.91 (s, 6H), 3.45 (t, J = 5.2 Hz, 2H), 4.37 (t, J = 4.8 Hz, 2H), 7.19 (d, 1H) , 7.82 (t, J = 7.6 Hz, 1H), 8.40 (d, 1H), 8.51(d, 1H), 8.58 (d, 1H). MS(ESI): m/z = 282.87 [M-H]⁻.

Synthesis of 4

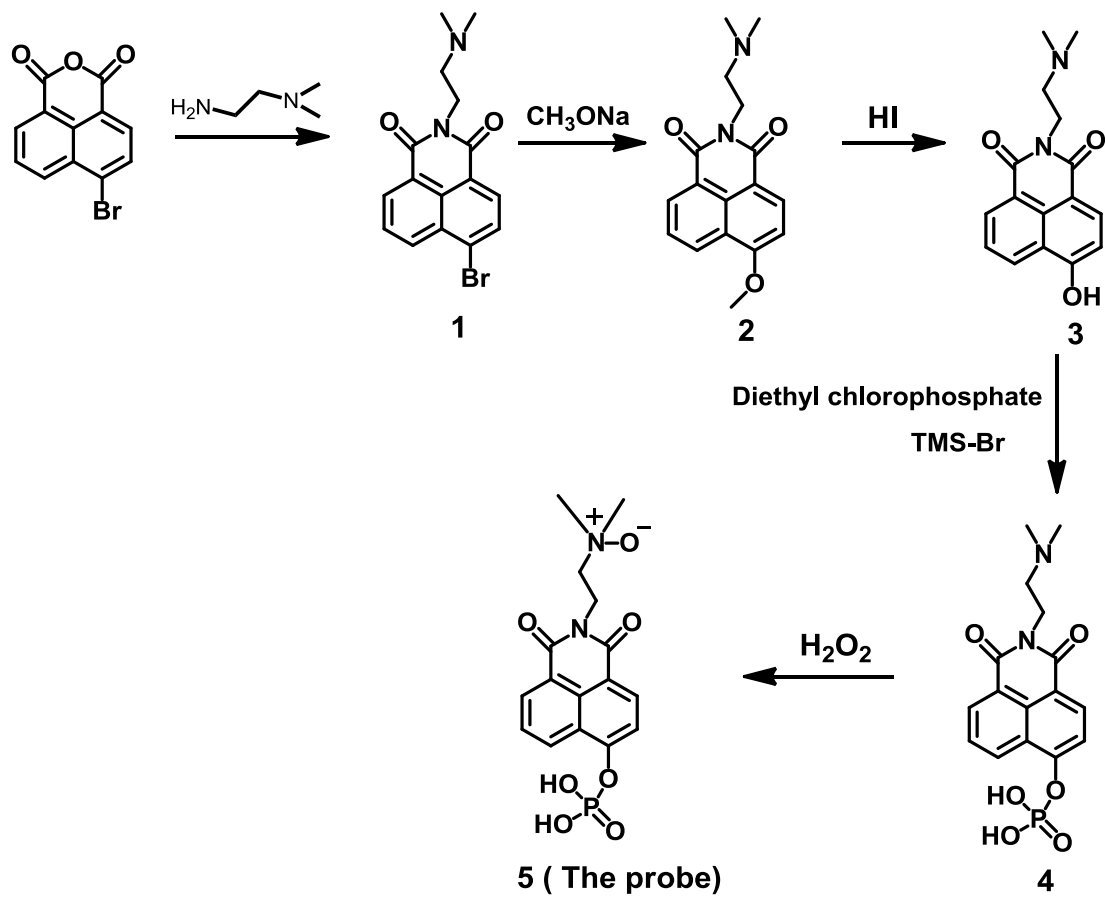
Under a nitrogen atmosphere, Compound **3** (71 mg, 0.25 mmol) and K₂CO₃ (345 mg, 2.5 mmol) were stirred in dichloromethane for 6 h. Then Diethyl chlorophosphate (55 μL, 0.375 mmol) was added and stirred overnight. Then TMS-Br (324 μL, 2.5 mmol) was added rapidly and stirred overnight. 10 mL methyl alcohol was added to quench the reaction. Then the solvent was evaporated and the residue was purified by column chromatography on silica gel (dichloromethane: methyl alcohol: ammonia water = 10: 10: 3 in v/v/v) to furnish the desired product (yield: 48%) as a white power. ¹H NMR (d6-DMSO, 400 MHz, ppm): 2.91 (s, 6H), 3.45 (t, J = 3.6 Hz, 2H), 4.37 (t, J = 4.0 Hz, 2H), 7.21 (d, 1H) , 7.81 (t, J = 4.8 Hz, 1H), 8.40 (d, 1H), 8.53 (d, 1H), 8.58 (d, 1H). ³¹P NMR (D₂O, 400 MHz, ppm): 2.69. MS (ESI): m/z = 363.90 [M-H]⁻

Synthesis of 5

Compound **4** (38 mg, 0.1 mmol) was dissolved in 15 mL 30% H₂O₂ aqueous solution and stirred overnight under a nitrogen atmosphere. Then the solvent was evaporated and the product was dried under vacuum at 50 °C for 48 h as a light yellow power (yield: 91%). ¹H NMR (D₂O, 400 MHz, ppm): 3.33 (s, 6H), 3.61 (t, J = 4.4 Hz, 2H),

4.46 (t, $J = 4.0$ Hz, 2H), 7.58-7.72 (m, 2H) , 8.30-8.40 (m, 2H), 8.58 (d, 1H). ^{31}P

NMR (D_2O , 400 MHz, ppm): 4.64. MS (ESI): $m/z = 378.01$ $[\text{M-H}]^-$.



Scheme S1. Synthetic route for the probe.

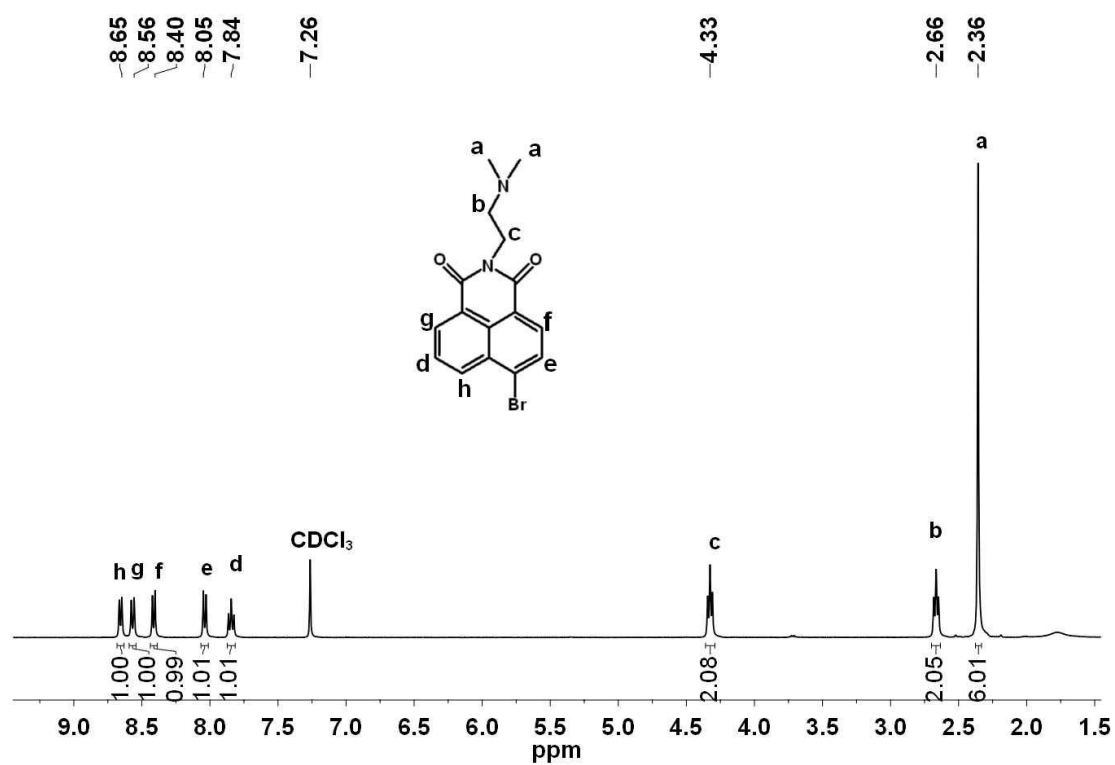


Figure S1. ¹H-NMR spectrum of 1.

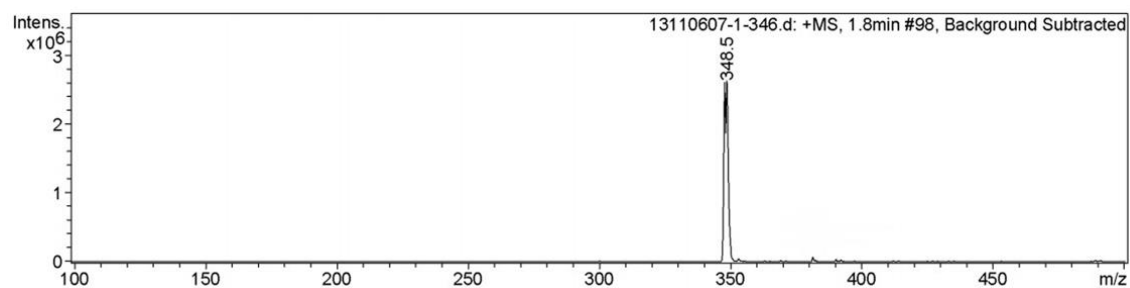


Figure S2. Mass spectrum of 1. MS(ESI): m/z 348.5 [M+H]⁺.

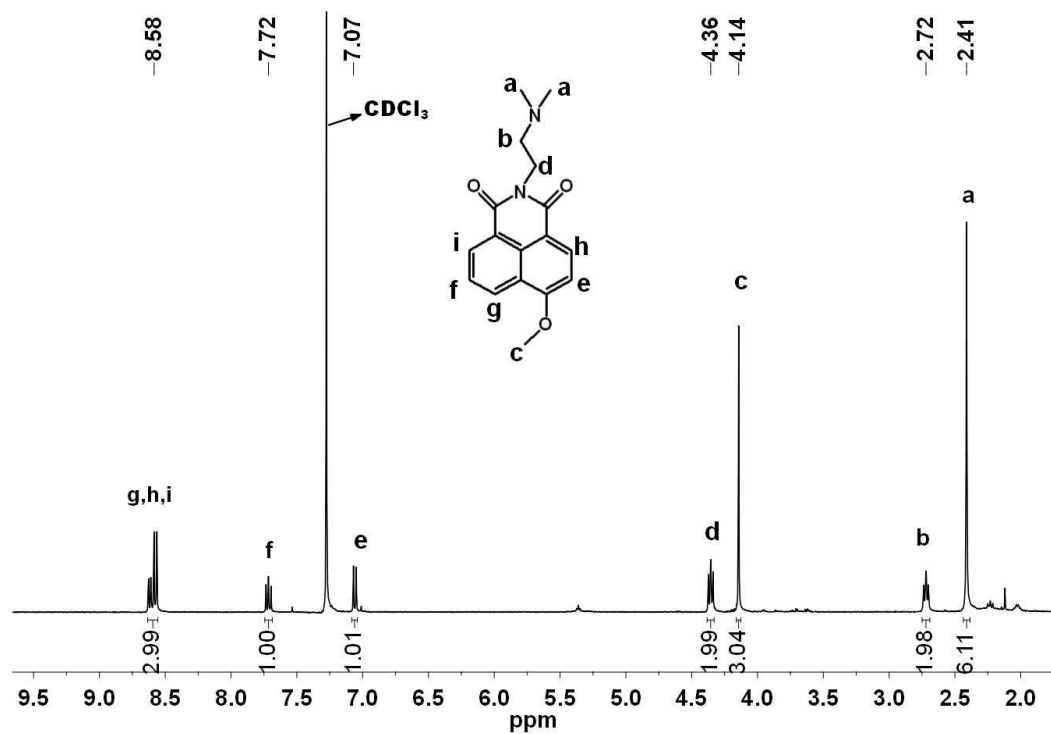


Figure S3. $^1\text{H-NMR}$ spectrum of **2**.

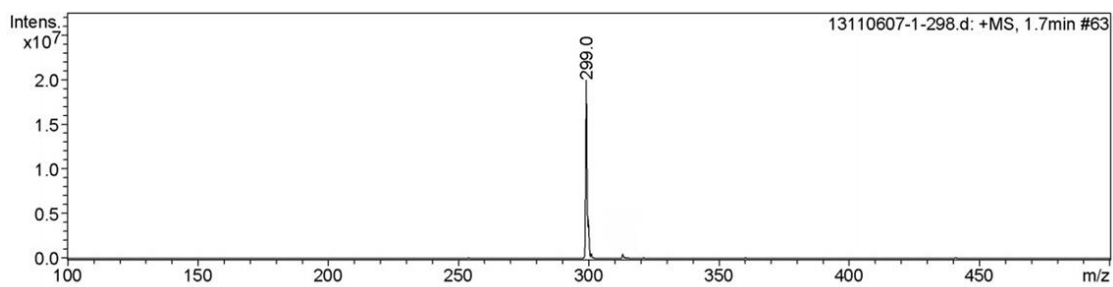


Figure S4. Mass spectrum of **2**. MS(ESI): m/z 299.0 $[\text{M}+\text{H}]^+$.

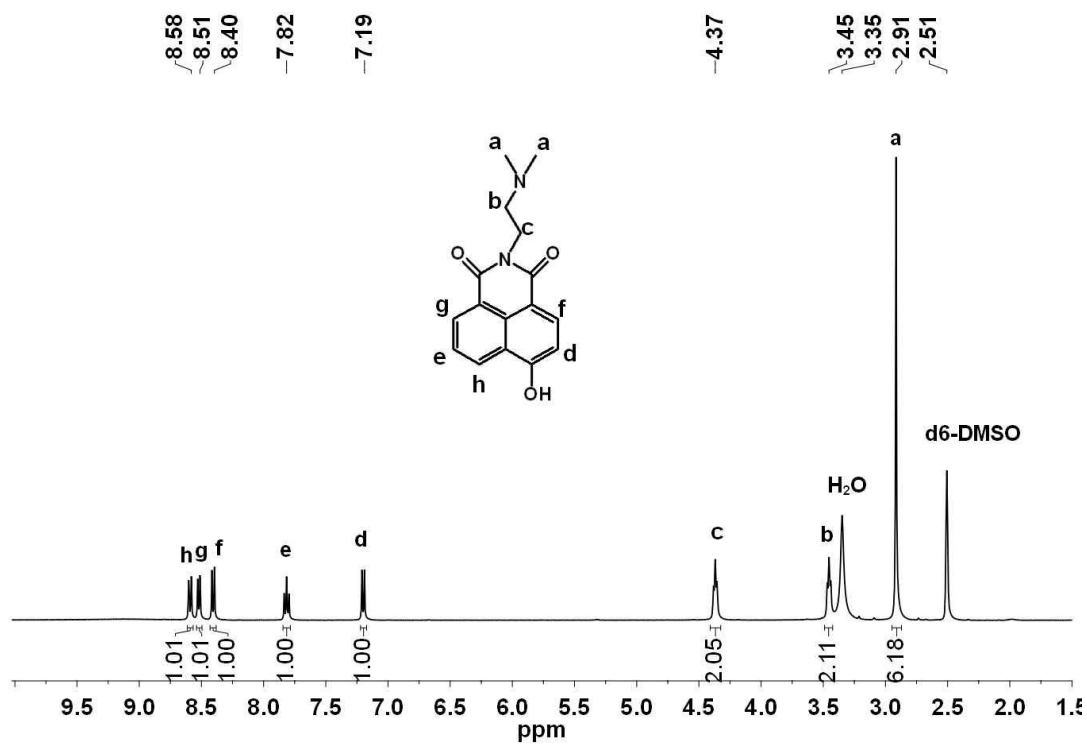


Figure S5. $^1\text{H-NMR}$ spectrum of **3**.

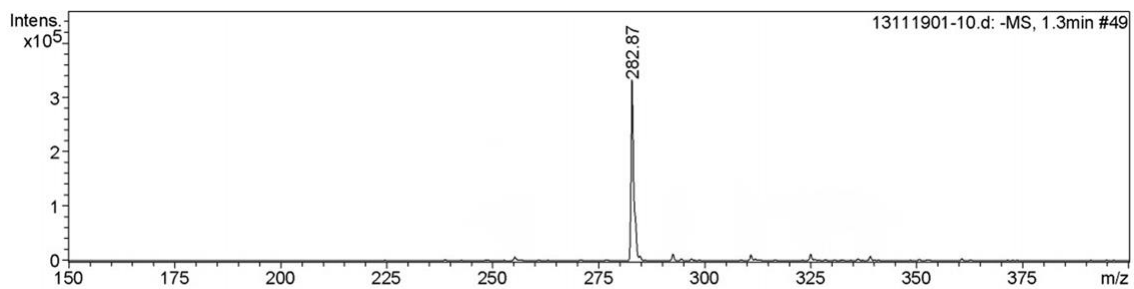


Figure S6. Mass spectrum of **3**. MS(ESI): m/z 282.87 $[\text{M-H}]^-$.

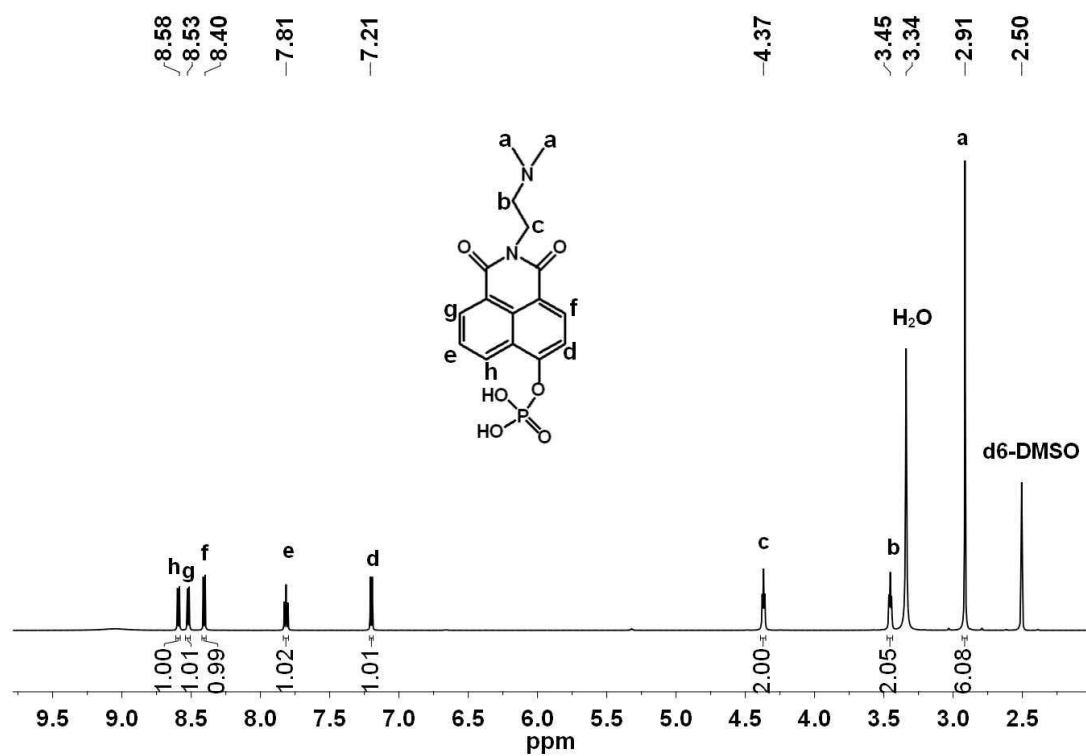


Figure S7. ^1H -NMR spectrum of 4.

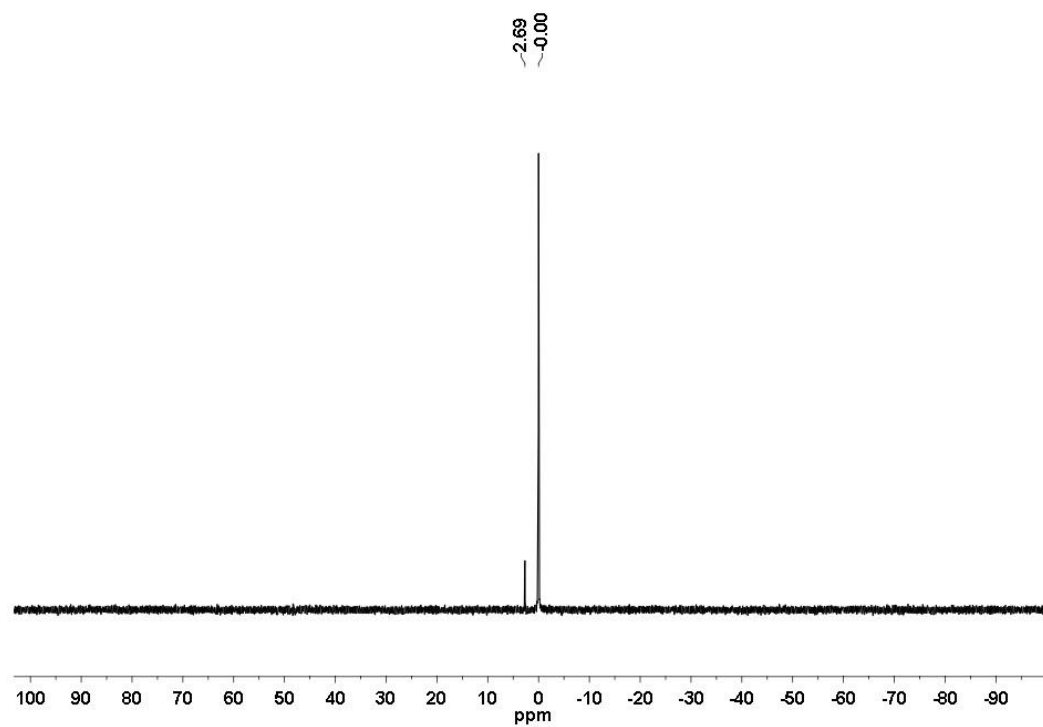


Figure S8. ^{31}P -NMR spectrum of 4.

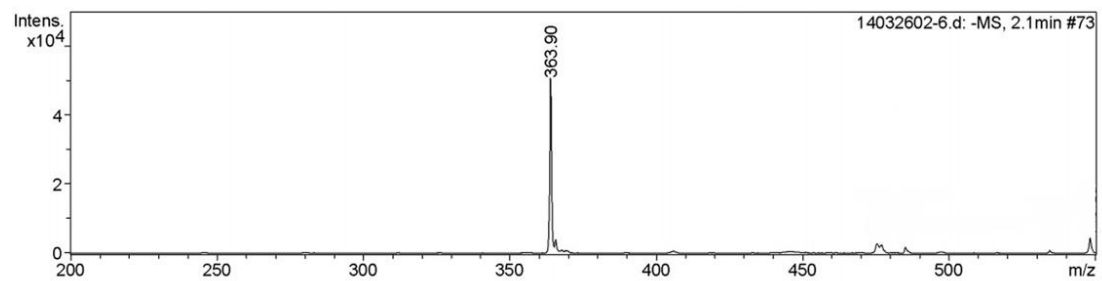


Figure S9. Mass spectrum of **4**. MS(ESI): m/z 363.90 $[M-H]^-$.

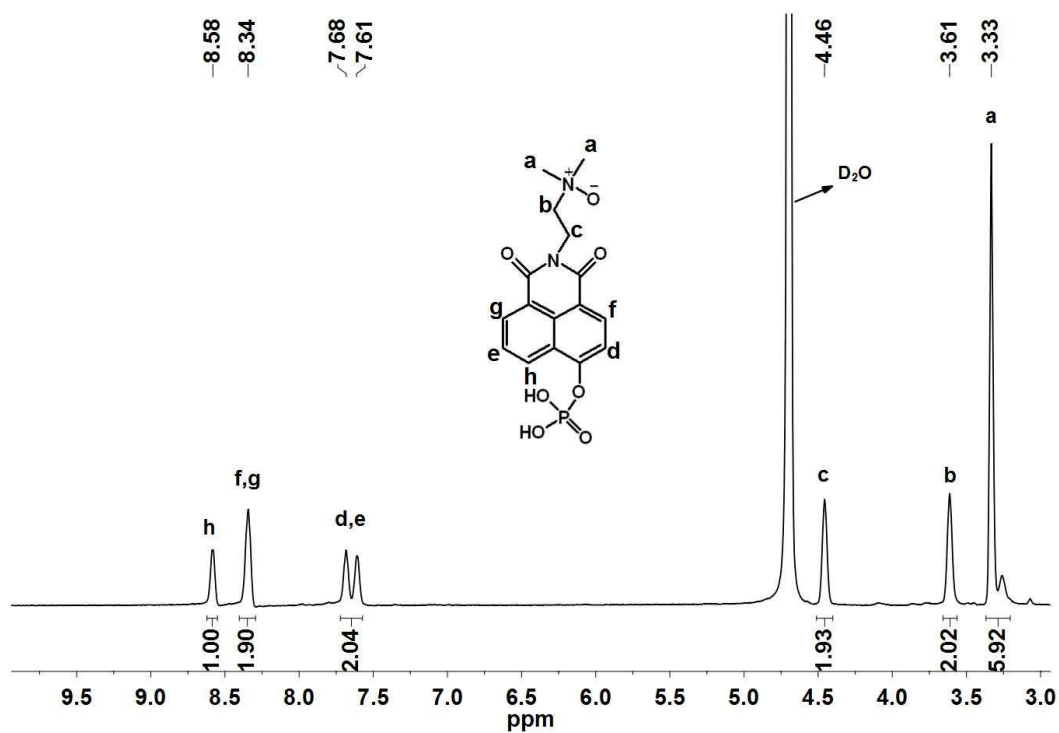


Figure S10. ^1H -NMR spectrum of 5.

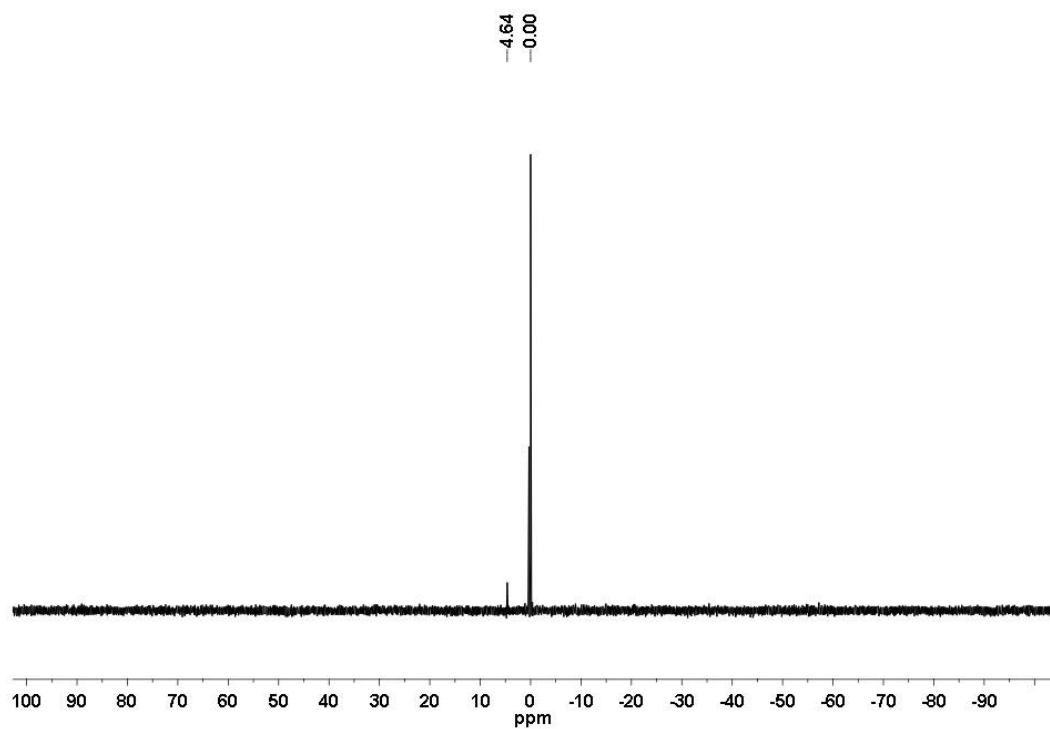


Figure S11. ^{31}P -NMR spectrum of 5.

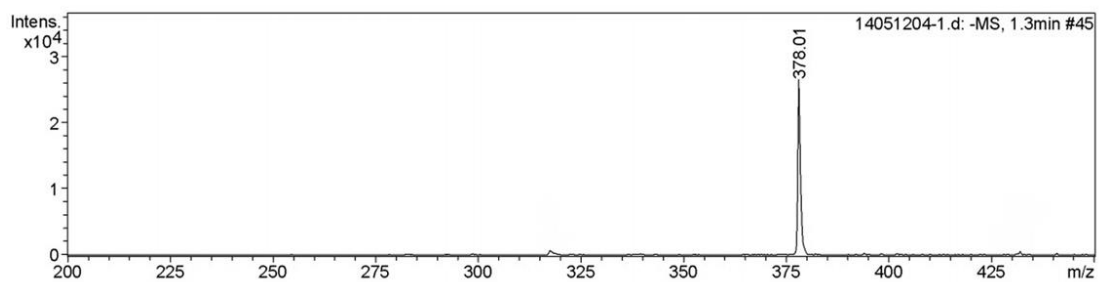


Figure S12. Mass spectrum of **5**. MS(ESI): m/z 378.01 [M-H]⁻.

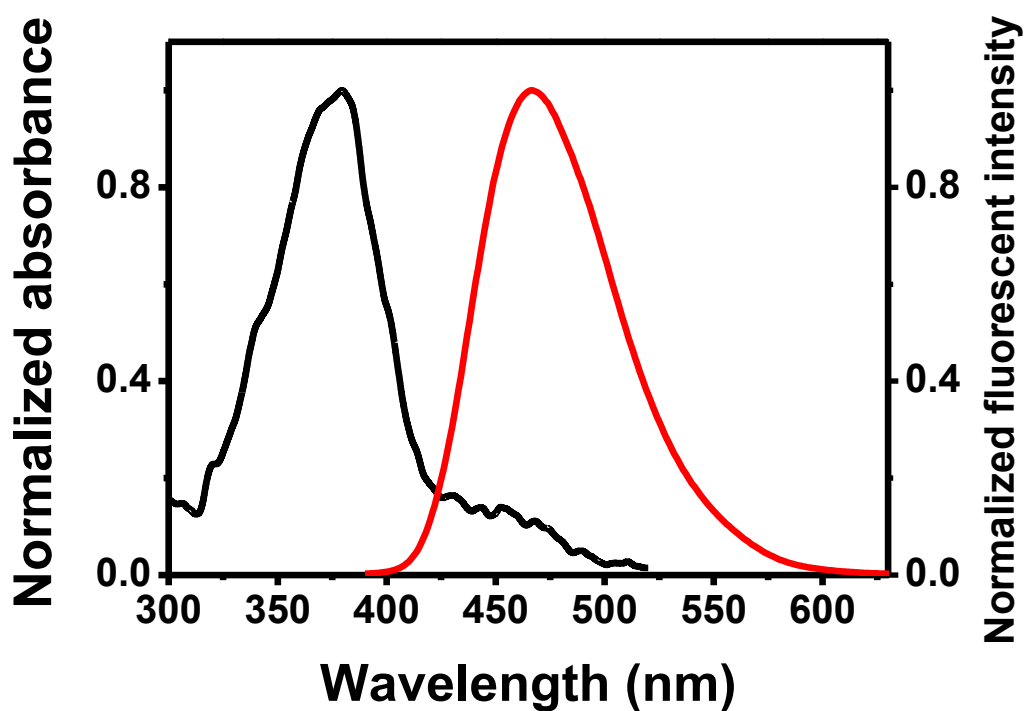


Figure S13. UV-vis absorption and fluorescence emission spectra ($\lambda_{ex} = 370$ nm) of the probe (5×10^{-6} M) in Tris-buffered (pH 8.0) water.

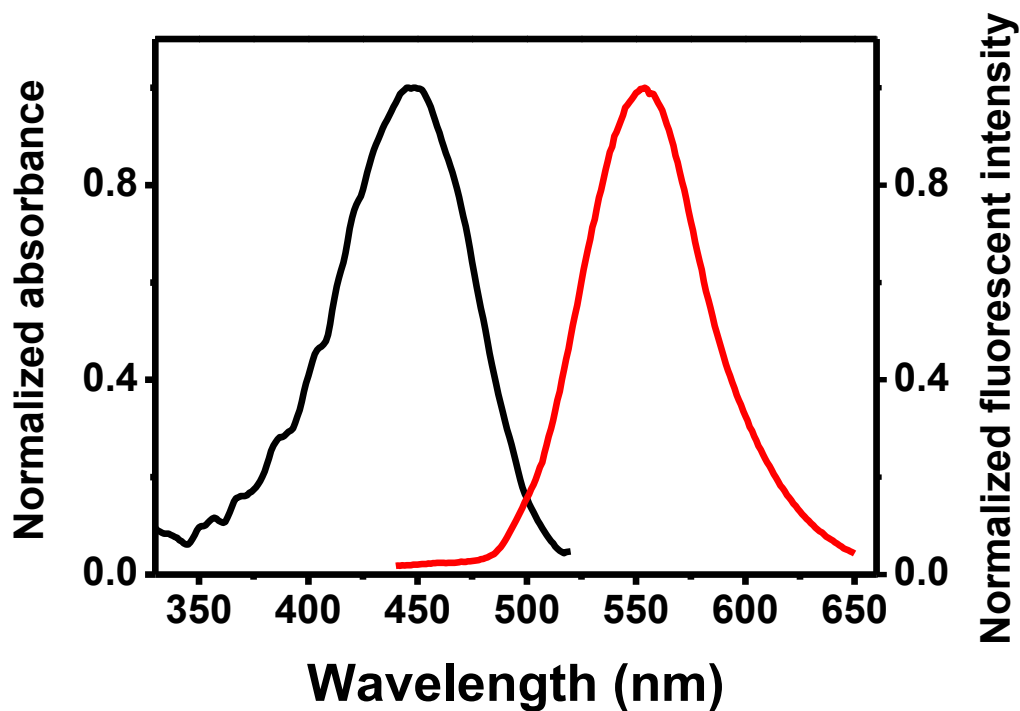


Figure S14. UV-vis absorption and fluorescence emission spectra ($\lambda_{ex} = 425$ nm) of the probe (5×10^{-6} M) upon being reacted with ALP in Tris-buffered (pH 8.0) water for 1 h at 37 °C.

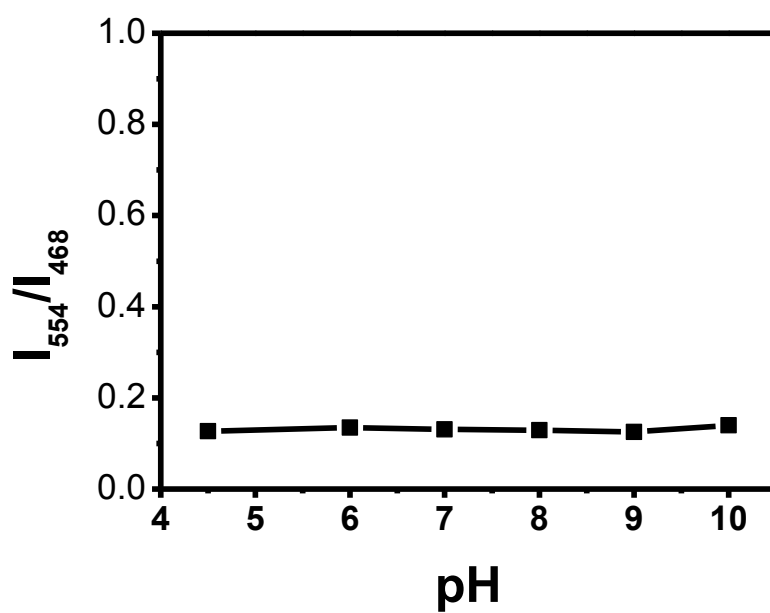


Figure S15. Stability of the probe under different pH values.

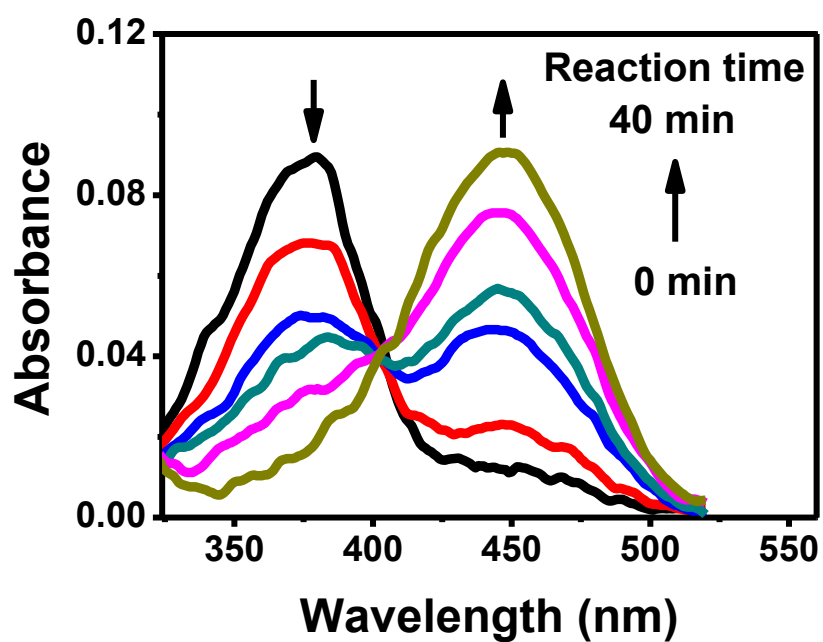


Figure S16. Absorption spectra of the probe as a function of reaction time in the presence of ALP (50 U/L) in Tris-HCl buffered (pH 8.0, 10 mM) water at 37°C.

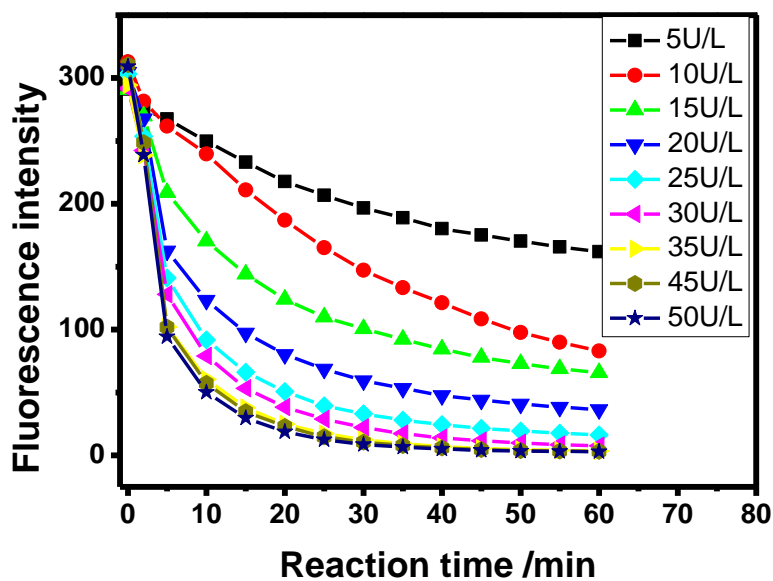


Figure S17. Fluorescence intensity at 468 nm of the probe (5×10^{-6} M) in Tris-HCl buffered (pH 8.0, 10 mM) water at 37°C versus reaction time in the presence of different amounts of ALP.

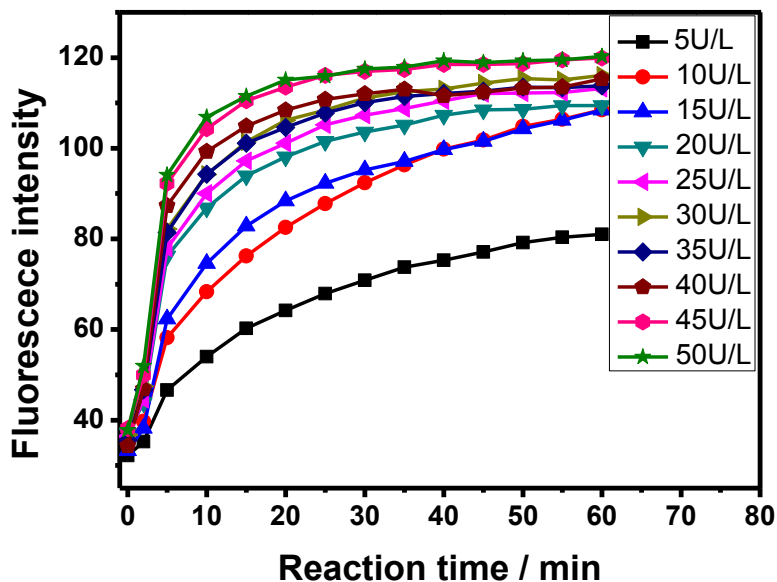


Figure S18. Fluorescence intensity at 554 nm of the probe (5×10^{-6} M) in Tris-HCl buffered (pH 8.0, 10 mM) water at 37°C versus reaction time in the presence of different amounts of ALP.

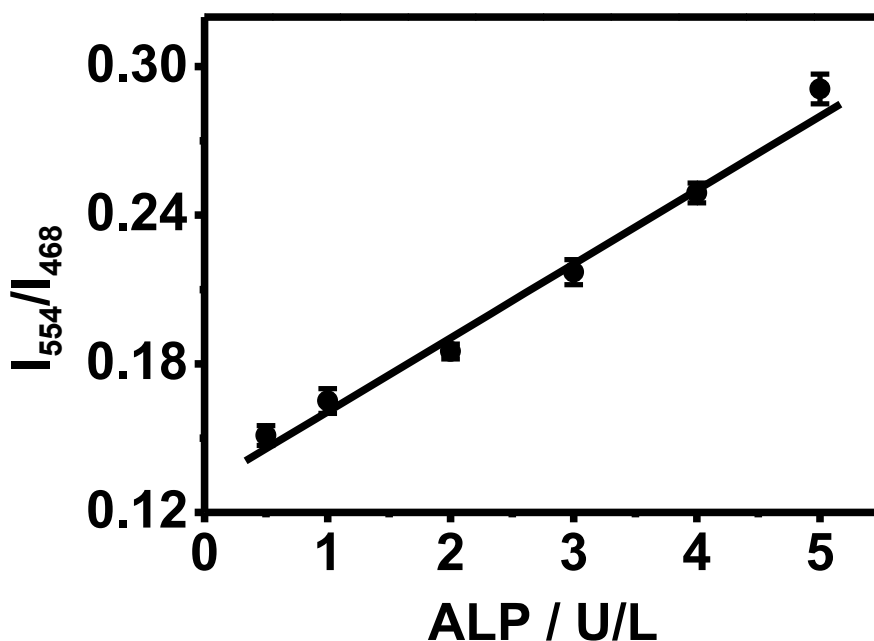


Figure S19. Fluorescence intensity ratio for the probe (5×10^{-6} M) in Tris-HCl buffered (pH 8.0, 10 mM) as a function of ALP level for 20 min. Excitation wavelength: 425 nm.

Determination of the detection limit:

First the calibration curve was obtained from the plot of fluorescence intensity ratio (I_{554}/I_{468}) as a function of the analyte concentration (ALP). The regression curve equation was then obtained for the lower concentration part.

The detection limit = $3 \times \text{S.D.} / k$

where k is the slope of the curve equation, and S.D. represents the standard deviation for the fluorescence intensity ratio of the probe in the absence of ALP.

$$I_{554}/I_{468} = 0.1311 + 0.0304 \times [\text{ALP}] \quad (R = 0.994)$$

$$\text{LOD} = 3 \times 0.00382 / 0.0304 = 0.38 \text{ U/L}$$

References:

V. Thomsen, D. Schatzlein and D. Mercurio, *Spectroscopy*, 2003, 18, 112-114.

A. D. McNaught and A. Wilkinson, *IUPAC Compendium of Chemical Terminology*, 1997.

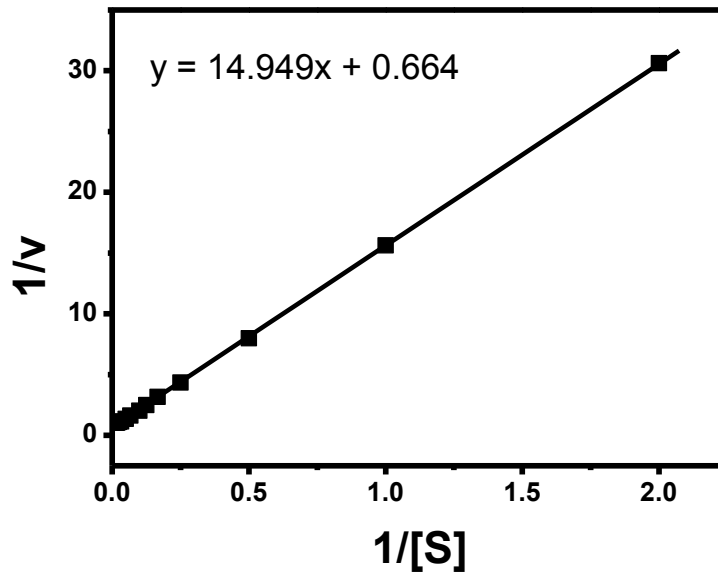
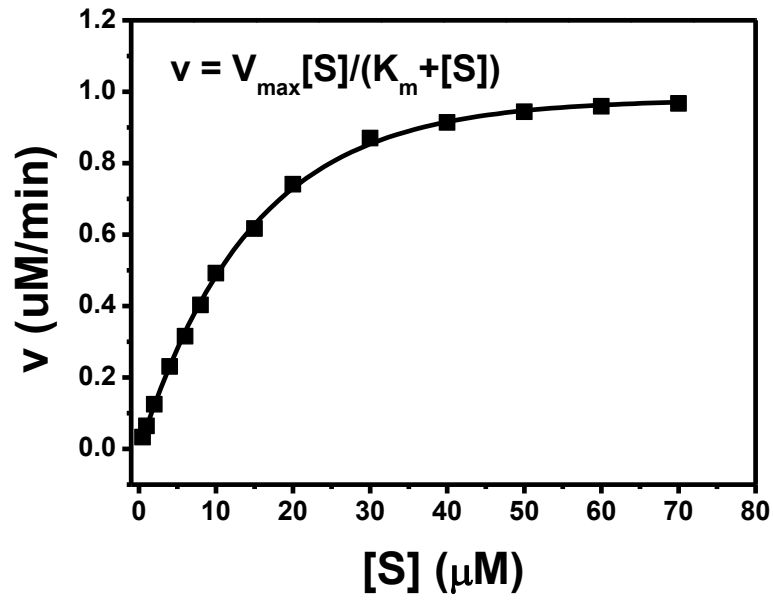
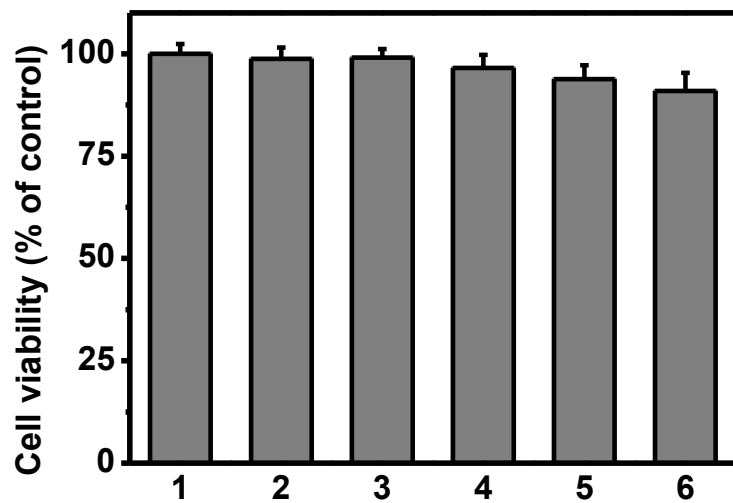
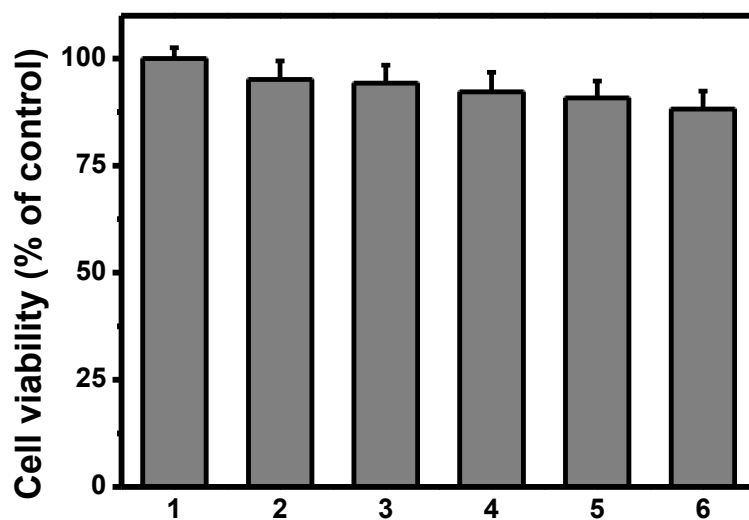


Figure S20. Substrate dependence of the initial degradation velocities for ALP. Initial velocities were plotted against the substrate concentrations and fit to the Michaelis-Menten model (The kinetic parameters: $V_{\max} = 1.506 \mu\text{M}/\text{min}$, $K_m = 22.514 \mu\text{M}$). Data show the means \pm SD from triplicate samples.



(A)



(B)

Figure S21. Cell viability for HeLa(A) and L929(B) cells in the presence of the probe at varied concentrations. The results are the mean standard deviation of eight separate measurements. 1-6 stand for mediums with the probe concentrations 0, 2×10^{-6} M, 5×10^{-6} M, 1×10^{-5} M, 2×10^{-5} M, 5×10^{-5} M.

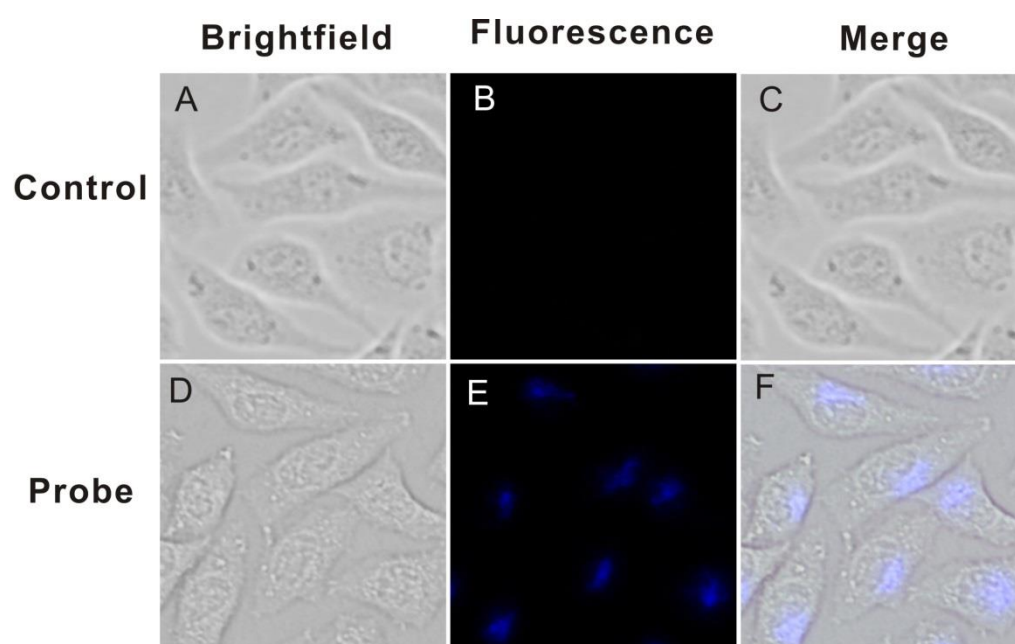


Figure S22. L929 cells incubated in the absence of the probe (A, B and C) or in the presence of the probe (D, E and F; the probe concentration: 1×10^{-5} M). (excitation filter 400 – 410 nm, emission filter ≥ 455 nm)

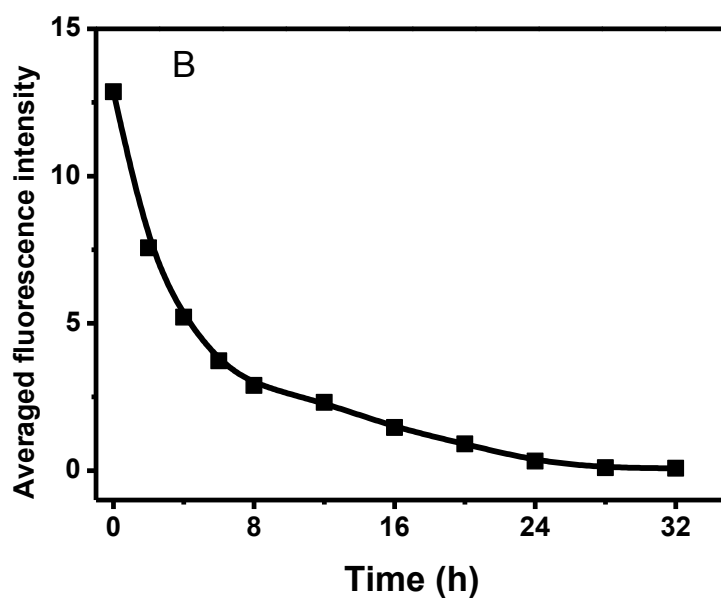
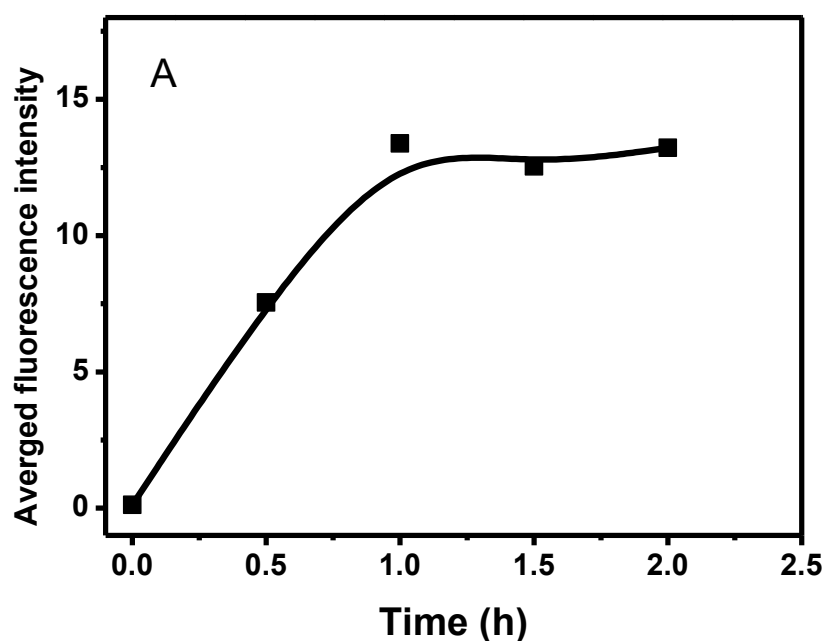


Figure S23. The averaged fluorescence intensity of zebrafishes for different incubation time periods. A: Averaged blue fluorescence intensity of the zebrafishes right after being incubated with the probe (2×10^{-5} M) for 0 h, 0.5 h, 1.5 h, 2 h respectively at 28 °C. B: Averaged blue fluorescence intensity of the zebrafishes at 0 h, 4 h, 12 h, 24 h upon being treated with the probe for 1 h and then incubated with E3 embryo media. Data were analyzed using Image Pro software.

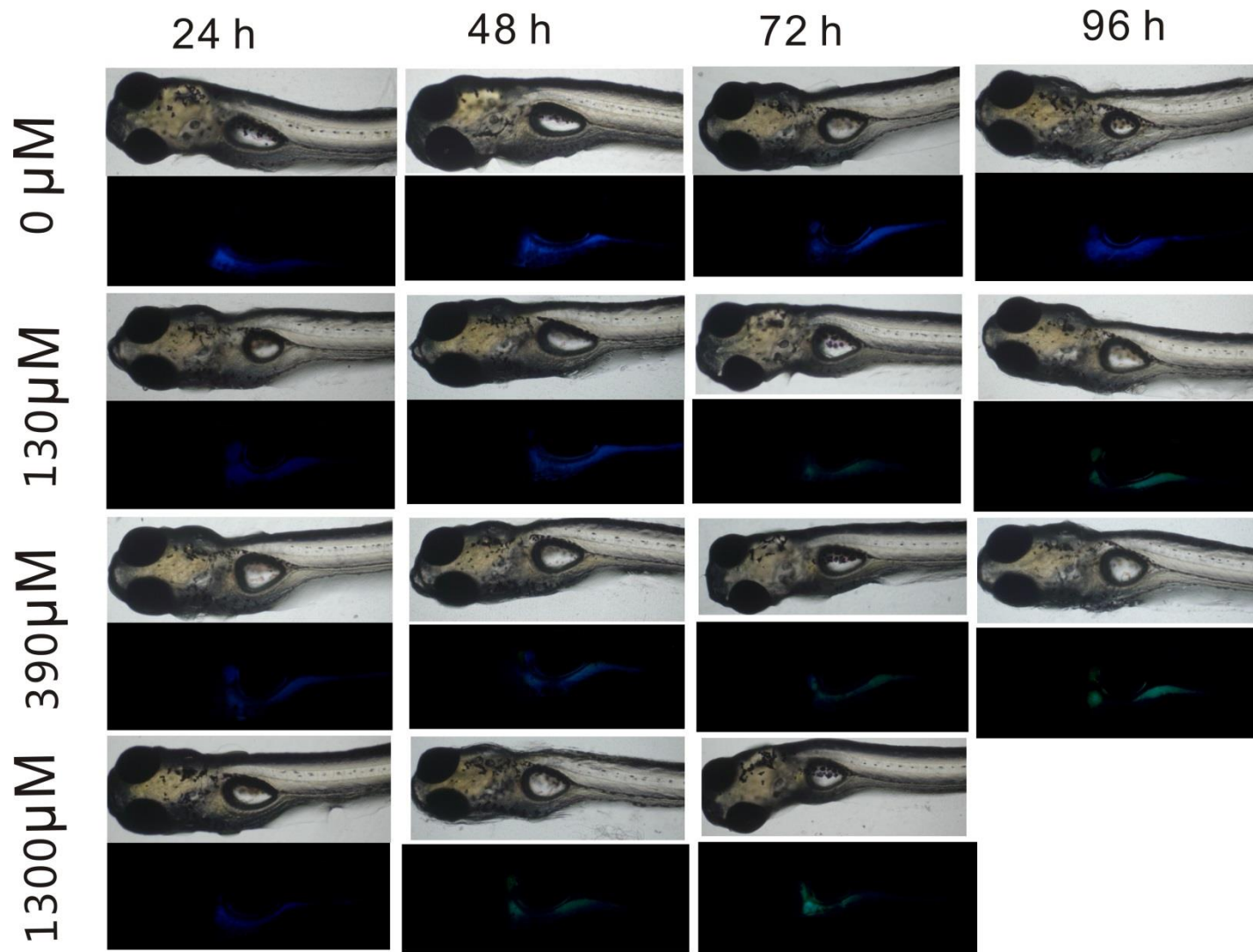


Figure S24. Fluorescent microscopy images of zebrafish larvae treated with different amounts of APAP for different time periods (Excitation filter 400 – 410 nm, emission filter \geq 455 nm).

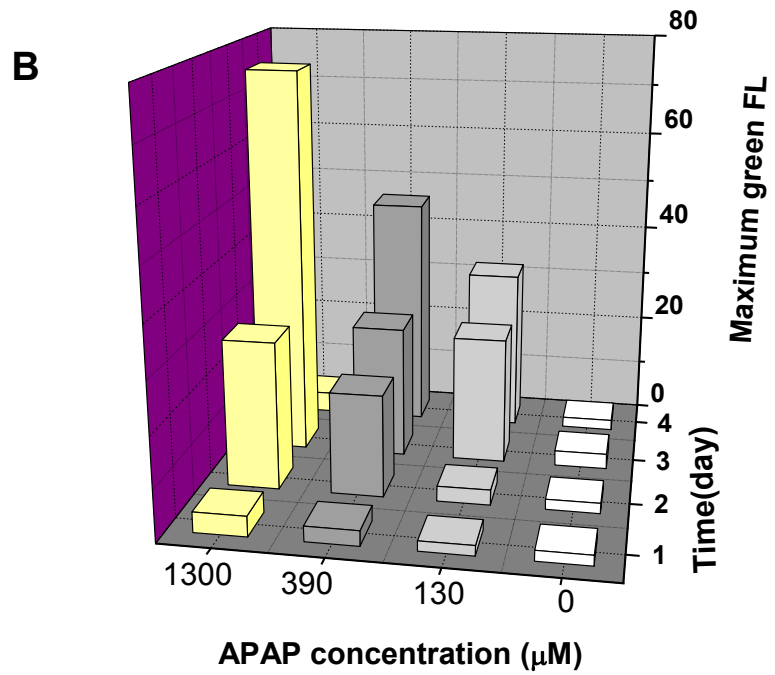
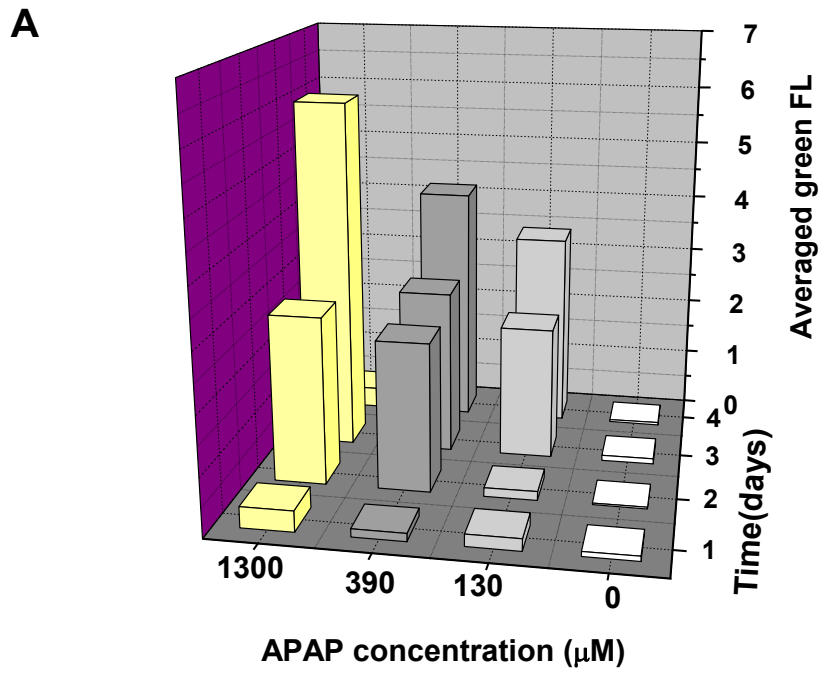


Figure S25. The averaged (A) and maximum (B) green fluorescence intensity of the zebrafishes upon being treated with different amounts of APAP for different time periods.

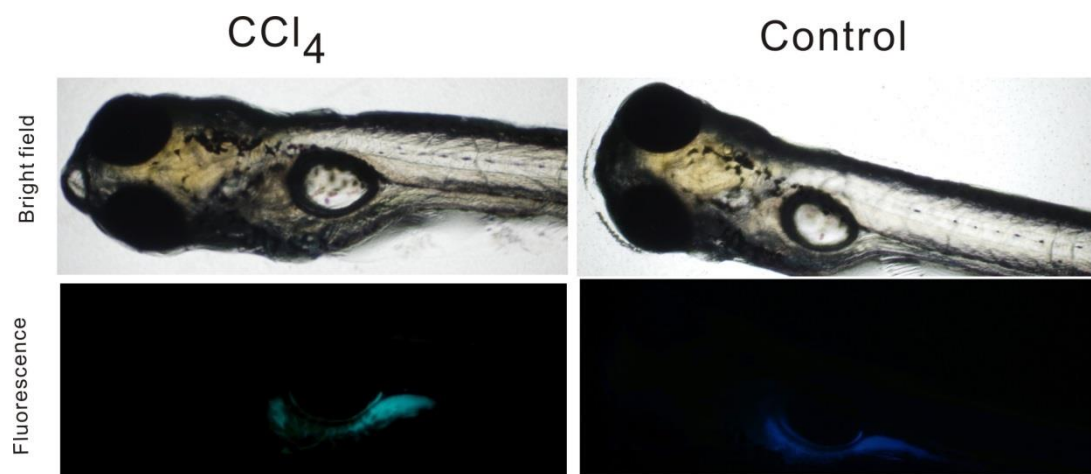


Figure S26. Fluorescence microscopy image of zebrafish larva treated with CCl₄ (800 mg/L) for 48 h and that without treatment of CCl₄ (the control). (Excitation filter 400 – 410 nm, emission filter \geq 455 nm)

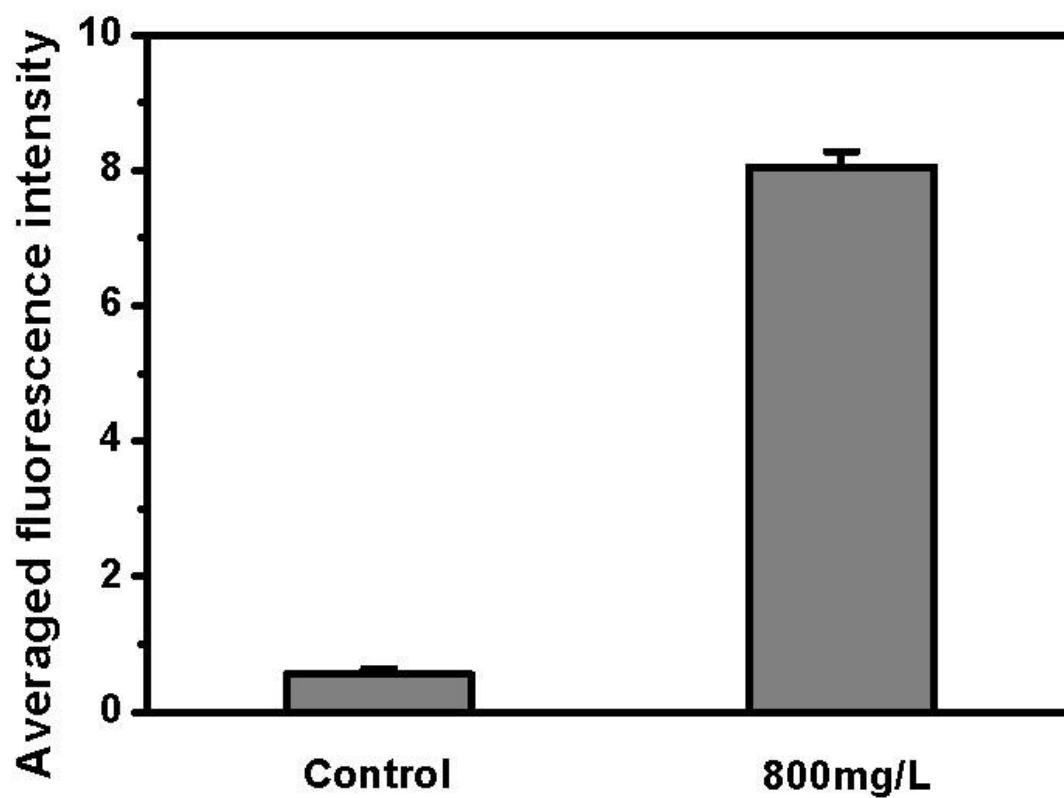


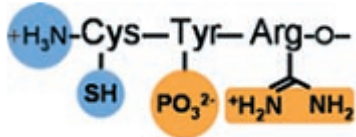
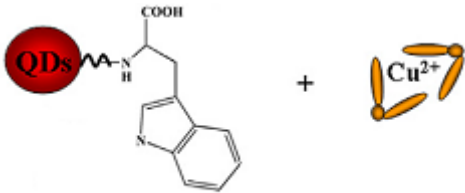
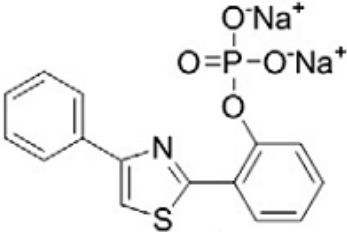
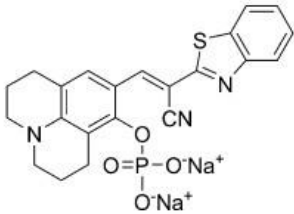
Figure S27. The average green fluorescence intensity of zebrafish larvae treated with CCl_4 (800 mg/L) for 48 h and those of zebrafish without treatment of CCl_4 (the control). Data were analyzed using Image Pro Plus software (NIH).

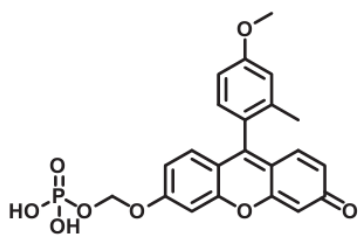
Table S1. ALP detection in human serum samples (positive and negative clinical samples) by using Elisa kit assay and this probe.

Sample No.	ELISA Kit assay ^[a]		This probe ^[b]	
	ALP level (U/L)	RSD(%)	ALP level (U/L)	RSD(%)
A ^[c]	56.8 ± 3.1	5.5	59.2 ± 2.2	3.7
B ^[c]	64.3 ± 2.5	3.9	66.1 ± 2.7	4.1
C ^[d]	238.7 ± 9.9	4.1	245.1 ± 7.8	3.2
D ^[d]	306.9 ± 11.4	3.7	303.9 ± 8.2	2.7

Note: [a] When ALP level was determined by using Elisa kit, the serum samples were 1000-fold diluted. [b] When ALP level was determined by using this probe, the serum samples were 10-fold diluted. [c] Negative clinical samples (serum samples from healthy males with normal ALP levels, as tested by the clinical laboratory of the Sixth Affiliated Hospital of Sun Yat-sen University). [d] Positive clinical samples (serum samples from males with abnormal ALP levels, as tested the clinical laboratory of the Sixth Affiliated Hospital of Sun Yat-sen University).

Table S2. Comparison of this probe with other reported probes for ALP.

Probe	Method	Applications	Comment
 <p>and Gold nanoparticles Angew. Chem. Int. Ed., 2007, 46, 707 –709</p>	Colorimetric	—	a quick and simply assay
Gold nanoparticles and ATP Biosensors and Bioelectronics, 2013,43, 366–371	Colorimetric	human serum samples	Simplicity in clinical practice
 <p>Biosensors and Bioelectronics, 2014,55, 249– 254</p>	Turn-off Fluorescent	human serum samples	Near-infrared
 <p>Bioorganic & Medicinal Chemistry Letters, 2012, 22, 5541–5544</p>	Turn-on Fluorescent	ALP-inhibitor	ESIPT mechanism
 <p>Chem. Commun., 2011, 47, 9825-9827</p>	Turn-on Fluorescent	In cells	Monitor endogenous ALP



Turn-on
Fluorescent

—

High selectivity

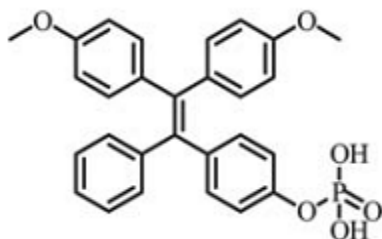
Bioorganic & Medicinal Chemistry
Letters, 2011, 21, 5088–5091

dsDNA, copper nanoparticles and
pyrophosphate
Anal. Chem., 2013, 85, 3797– 3801

Turn-on
Fluorescent

human serum
samples

convenient

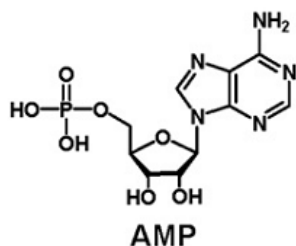


Turn-on
Fluorescent

in cells

AIE mechanism

Analyst, 2013, 138 , 2427

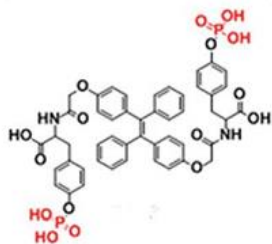


Turn-off
Fluorescent

—

sensing of
adenosine &
ALP

and S-adenosylhomocysteine
Biosensors and Bioelectronics, 2013, 41,
379–385

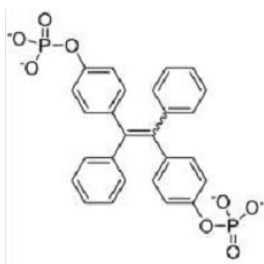


Turn-on
Fluorescent

in cells

AIE
mechanism;
multifunctional
properties

J. Mater. Chem. B, 2013, 1, 5550–5556

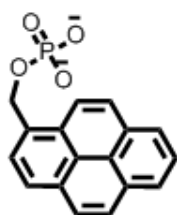


Turn-on
Fluorescent

in fetal
bovine
serum
samples

AIE
mechanism;
a long linear
range

ACS Appl. Mater. Interfaces, 2013, 5, 8784 –
8789



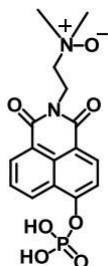
Ratiometric
Fluorescent

human serum
samples

better
performance
than ALP
ELISA Kit

and betaine-modified PEI

Anal. Chem., 2014, 86, 9873–9879



This work

Ratiometric
Fluorescent

human serum
samples;
in cells;
in vivo

Ratiometric
mode;
tracking
endogenous
ALP in vivo

References:

- [1] Y. Choi, N.-H. Ho and C.-H. Tung, *Angew. Chem. Int. Ed.*, 2007, **46**, 707–709.
 [2] C. M. Li, S. J. Zhen, J. Wang, Y. F. Li and C. Z. Huang, *Biosensors and Bioelectronics*, 2013, **43**, 366–371.
 [3] S. Liu, S. Pang, W. Na and X. Su, *Biosensors and Bioelectronics*, 2014, **55**, 249–254.

- [4] J. Park, A. Helal, H.-S. Kim and Y. Kim, *Bioorganic & Medicinal Chemistry Letters*, 2012, **22**, 5541–5544.
- [5] T.-I. Kim, H. Kim, Y. Choi and Y. Kim, *Chem. Commun.*, 2011, **47**, 9825–9827.
- [6] M. Kawaguchi, K. Hanaoka, T. Komatsu, T. Terai and T. Nagano, *Bioorganic & Medicinal Chemistry Letters*, 2011, **21**, 5088–5091.
- [7] L. Zhang, J. Zhao, M. Duan, H. Zhang, J. Jiang and R. Yu, *Anal. Chem.*, 2013, **85**, 3797–3801.
- [8] X. Gu, G. Zhang, Z. Wang, W. Liu, L. Xiao and D. Zhang, *Analyst*, 2013, **138**, 2427–2431.
- [9] J.-H. Lin and W.-L. Tseng, *Biosensors and Bioelectronics*, 2013, **41**, 379–385.
- [10] H. Liu, Z. Lv, K. Ding, X. Liu, L. Yuan, H. Chen and X. Li, *J. Mater. Chem. B*, 2013, **1**, 5550–5556.
- [11] J. Liang, R. T. K. Kwok, H. Shi, B. Z. Tang and B. Liu, *ACS Appl. Mater. Interfaces*, 2013, **5**, 8784–8789.
- [12] F. Zheng, S. Guo, F. Zeng, J. Li and S. Wu, *Anal. Chem.*, 2014, **86**, 9873–9879.